Silicon-organic hybrid (SOH) frequency comb sources for terabit/s data transmission

C. Weimann,[1,*] P. C. Schindler,[1] R. Palmer,[1] S. Wolf,[1] D. Bekele,[1] D. Korn,[1] J. Pfeifle,[1] S. Koeber,[1] R. Schmogrow,[1] L. Alloatti,[1] D. Elder,[2] H. Yu,[3] W. Bogaerts,[3] L. R. Dalton,[2] W. Freude,[1] J. Leuthold,[1,4] and C. Koos[1,5]

[1]*Karlsruhe Institute of Technology (KIT), Institute of Photonics and Quantum Electronics (IPQ) and Institute of Microstructure Technology (IMT), 76131 Karlsruhe, Germany*
[2]*University of Washington, Department of Chemistry, Seattle, WA 98195-1700, USA*
[3]*Ghent University – IMEC, Photonics Research Group, Gent, Belgium*
[4]*Electromagnetic Fields & Microwave Electronics Laboratory (IFH), ETH-Zurich, Zurich, Switzerland*
[5]*christian.koos@kit.edu*
[*]*claudius.weimann@kit.edu*

Abstract: We demonstrate frequency comb sources based on silicon-organic hybrid (SOH) electro-optic modulators. Frequency combs with line spacings of 25 GHz and 40 GHz are generated, featuring flat-top spectra with less than 2 dB power variations over up to 7 lines. The combs are used for WDM data transmission at terabit/s data rates and distances of up to 300 km.

OCIS codes: (130.3120) Integrated optics devices; (060.4510) Optical communications.

References and links

1. I. Coddington, W. C. Swann, L. Nenadovic, and N. R. Newbury, "Rapid and precise absolute distance measurements at long range," Nat. Photonics **3**(6), 351–356 (2009).
2. S. T. Cundiff and A. M. Weiner, "Optical arbitrary waveform generation," Nat. Photonics **4**(11), 760–766 (2010).
3. D. Hillerkuss, R. Schmogrow, T. Schellinger, M. Jordan, M. Winter, G. Huber, T. Vallaitis, R. Bonk, P. Kleinow, F. Frey, M. Roeger, S. Koenig, A. Ludwig, A. Marculescu, J. Li, M. Hoh, M. Dreschmann, J. Meyer, S. Ben Ezra, N. Narkiss, B. Nebendahl, F. Parmigiani, P. Petropoulos, B. Resan, A. Oehler, K. Weingarten, T. Ellermeyer, J. Lutz, M. Moeller, M. Huebner, J. Becker, C. Koos, W. Freude, and J. Leuthold, "26 Tbit/s line-rate super-channel transmission utilizing all-optical fast Fourier transform processing," Nat. Photonics **5**(6), 364–371 (2011).
4. Y.-K. Huang, E. Ip, Z. Wang, M.-F. Huang, Y. Shao, and T. Wang, "Transmission of spectral efficient super-channels using all-optical OFDM and digital coherent receiver technologies," J. Lightwave Technol. **29**(24), 3838–3844 (2011).
5. T. Sakamoto, T. Kawanishi, and M. Izutsu, "Asymptotic formalism for ultraflat optical frequency comb generation using a Mach-Zehnder modulator," Opt. Lett. **32**(11), 1515–1517 (2007).
6. L. Gheorma, G. K. Gopalakrishnan, "Flat frequency comb generation with an integrated dual-parallel modulator," IEEE Photonics Technol. Lett. **19**(13), 1011–1013 (2007).
7. S. Ozharar, F. Quinlan, I. Ozdur, S. Gee, and P. Delfyett, "Ultraflat optical comb generation by phase-only modulation of continuous-wave light," IEEE Photonics Technol. Lett. **20**(1), 36–38 (2008).
8. J. Veselka and S. Korotky, "A multiwavelength source having precise channel spacing for WDM systems," IEEE Photonics Technol. Lett. **10**(7), 958–960 (1998).
9. R. Wu, V. R. Supradeepa, C. M. Long, D. E. Leaird, and A. M. Weiner, "Generation of very flat optical frequency combs from continuous-wave lasers using cascaded intensity and phase modulators driven by tailored radio frequency waveforms," Opt. Lett. **35**(19), 3234–3236 (2010).
10. T. Healy, F. C. Garcia Gunning, A. D. Ellis, and J. D. Bull, "Multi-wavelength source using low drive-voltage amplitude modulators for optical communications," Opt. Express **15**(6), 2981–2986 (2007).
11. A. Metcalf, V. Torres-Company, D. Leaird, and A. Weiner, "High-power broadly tunable electro-optic frequency comb generator," IEEE J. Sel. Top. Quantum Electron. **19**(6), 3500306 (2013).
12. J. Zhang, J. Yu, Z. Dong, Y. Shao, and N. Chi, "Generation of full C-band coherent and frequency-lock multi-carriers by using recirculating frequency shifter loops based on phase modulator with external injection," Opt. Express **19**(27), 26370–26381 (2011).
13. K.-P. Ho and J. Kahn, "Optical frequency comb generator using phase modulation in amplified circulating loop," IEEE Photonics Technol. Lett. **5**(6), 721–725 (1993).
14. N. Dupuis, C. R. Doerr, L. Zhang, L. Chen, N. J. Sauer, P. Dong, L. L. Buhl, and D. Ahn, "InP-based comb generator for optical OFDM," J. Lightwave Technol. **30**(4), 466–472 (2012).

15. T. Sakamoto, T. Kawanishi, and M. Izutsu, "Widely wavelength-tunable ultra-flat frequency comb generation using conventional dual-drive Mach-Zehnder modulator," Electron. Lett. **43**(19), 1039 (2007).
16. A. Biberman and K. Bergman, "Optical interconnection networks for high-performance computing systems," Rep. Prog. Phys. **75**(4), 046402 (2012).
17. D. J. Thomson, F. Y. Gardes, J.-M. Fedeli, S. Zlatanovic, Y. Hu, B. P. P. Kuo, E. Myslivets, N. Alic, S. Radic, G. Z. Mashanovich, and G. T. Reed, "50-Gb/s silicon optical modulator," IEEE Photonics Technol. Lett. **24**(4), 234–236 (2012).
18. L. Liao, A. Liu, J. Basak, H. Nguyen, M. Paniccia, D. Rubin, Y. Chetrit, R. Cohen, and N. Izhaky, "40 Gbit/s silicon optical modulator for highspeed applications," Electron. Lett. **43**(22), 1196 (2007).
19. M. Watts, W. Zortman, D. Trotter, R. Young, and A. Lentine, "Low-voltage, compact, depletion-mode, silicon Mach-Zehnder modulator," IEEE J. Sel. Top. Quantum Electron. **16**(1), 159–164 (2010).
20. W. M. Green, M. J. Rooks, L. Sekaric, and Y. A. Vlasov, "Ultra-compact, low RF power, 10 Gb/s silicon Mach-Zehnder modulator," Opt. Express **15**(25), 17106–17113 (2007).
21. T. W. Baehr-Jones and M. J. Hochberg, "Polymer silicon hybrid systems: A platform for practical nonlinear optics," J. Phys. Chem. C **112**(21), 8085–8090 (2008).
22. J. H. Wülbern, S. Prorok, J. Hampe, A. Petrov, M. Eich, J. Luo, A. K.-Y. Jen, M. Jenett, and A. Jacob, "40 GHz electro-optic modulation in hybrid silicon-organic slotted photonic crystal waveguides," Opt. Lett. **35**(16), 2753–2755 (2010).
23. J.-M. Brosi, C. Koos, L. C. Andreani, M. Waldow, J. Leuthold, and W. Freude, "High-speed low-voltage electro-optic modulator with a polymer-infiltrated silicon photonic crystal waveguide," Opt. Express **16**(6), 4177–4191 (2008).
24. R. Ding, T. Baehr-Jones, W.-J. Kim, A. Spott, M. Fournier, J.-M. Fedeli, S. Huang, J. Luo, A. K.-Y. Jen, L. Dalton, and M. Hochberg, "Sub-volt silicon-organic electro-optic modulator with 500 Mhz bandwidth," J. Lightwave Technol. **29**(8), 1112–1117 (2011).
25. M. Hochberg, T. Baehr-Jones, G. Wang, J. Huang, P. Sullivan, L. Dalton, and A. Scherer, "Towards a millivolt optical modulator with nano-slot waveguides," Opt. Express **15**(13), 8401–8410 (2007).
26. L. Alloatti, D. Korn, R. Palmer, D. Hillerkuss, J. Li, A. Barklund, R. Dinu, J. Wieland, M. Fournier, J. Fedeli, H. Yu, W. Bogaerts, P. Dumon, R. Baets, C. Koos, W. Freude, and J. Leuthold, "42.7 Gbit/s electro-optic modulator in silicon technology," Opt. Express **19**(12), 11841–11851 (2011).
27. C. Weimann, S. Wolf, D. Korn, R. Palmer, S. Koeber, R. Schmogrow, P. C. Schindler, L. Alloatti, A. Ludwig, W. Heni, D. Bekele, D. L. Elder, H. Yu, W. Bogaerts, L. R. Dalton, W. Freude, J. Leuthold, and C. Koos, "Silicon-organic hybrid (SOH) frequency comb source for data transmission at 784 Gbit/s," in *European Conference and Exhibition on Optical Communication (ECOC)* (Optical Society of America, 2013), paper Th.2.B.1.
28. R. Palmer, L. Alloatti, D. Korn, P. Schindler, M. Baier, J. Bolten, T. Wahlbrink, M. Waldow, R. Dinu, W. Freude, C. Koos, and J. Leuthold, "Low power Mach-Zehnder modulator in silicon-organic hybrid technology," IEEE Photonics Technol. Lett. **25**(13), 1226–1229 (2013).
29. V. R. Almeida, Q. Xu, C. A. Barrios, and M. Lipson, "Guiding and confining light in void nanostructure," Opt. Lett. **29**(11), 1209–1211 (2004).
30. R. Palmer, S. Koeber, W. Heni, D. Elder, D. Korn, H. Yu, L. Alloatti, S. Koenig, P. Schindler, W. Bogaerts, M. Pantouvaki, G. Lepege, O. Verheyen, J. Van Campenhout, P. Absil, R. Baets, L. Dalton, W. Freude, J. Leuthold, and C. Koos, "High-speed silicon-organic hybrid (SOH) modulator with 1.6 fJ/bit and 180 pm/V in-device nonlinearity," in *European Conference and Exhibition on Optical Communication (ECOC)* (Optical Society of America, 2013), paper We.3.B.3.
31. D. Taillaert, F. van Laere, M. Ayre, W. Bogaerts, D. van Thourhout, P. Bienstman, and R. Baets, "Grating couplers for coupling between optical fibers and nanophotonic waveguides," Jpn. J. Appl. Phys. **45**(8A), 6071–6077 (2006).
32. R. Schmogrow, M. Winter, M. Meyer, D. Hillerkuss, S. Wolf, B. Baeuerle, A. Ludwig, B. Nebendahl, S. Ben-Ezra, J. Meyer, M. Dreschmann, M. Huebner, J. Becker, C. Koos, W. Freude, and J. Leuthold, "Real-time Nyquist pulse generation beyond 100 Gbit/s and its relation to OFDM," Opt. Express **20**(1), 317–337 (2012).
33. R. Schmogrow, D. Hillerkuss, M. Dreschmann, M. Huebner, M. Winter, J. Meyer, B. Nebendahl, C. Koos, J. Becker, W. Freude, and J. Leuthold, "Real-time Software-defined multiformat transmitter generating 64QAM at 28 GBd," IEEE Photonics Technol. Lett. **22**(21), 1601–1603 (2010).
34. F. Chang, K. Onohara, and T. Mizuochi, "Forward error correction for 100 G transport networks," IEEE Commun. Mag. **48**(3), S48–S55 (2010).
35. ITU, "Spectral grids for WDM applications: DWDM frequency grid," (ITU-T Recommendation G.694.1), International Telecommunications Union, February 2012, http://www.itu.int/rec/T-REC-G.694.1/.
36. D. Hillerkuss, R. Schmogrow, M. Meyer, S. Wolf, M. Jordan, P. Kleinow, N. Lindenmann, P. C. Schindler, A. Melikyan, X. Yang, S. Ben-Ezra, B. Nebendahl, M. Dreschmann, J. Meyer, F. Parmigiani, P. Petropoulos, B. Resan, A. Oehler, K. Weingarten, L. Altenhain, T. Ellermeyer, M. Moeller, M. Huebner, J. Becker, C. Koos, W. Freude, and J. Leuthold, "Single-laser 32.5 Tbit/s Nyquist WDM transmission," J. Opt. Commun. Netw. **4**(10), 715–723 (2012).
37. R. Schmogrow, B. Nebendahl, M. Winter, A. Josten, D. Hillerkuss, S. Koenig, J. Meyer, M. Dreschmann, M. Huebner, C. Koos, J. Becker, W. Freude, and J. Leuthold, "Error vector magnitude as a performance measure for advanced modulation formats," IEEE Photonics Technol. Lett. **24**(1), 61–63 (2012).
38. J. Luo, S. Huang, Z. Shi, B. M. Polishak, X.-H. Zhou, and A. K. Jen, "Tailored organic electro-optic materials and their hybrid systems for device applications," Chem. Mater. **23**(3), 544–553 (2011).

#200735 - $15.00 USD Received 7 Nov 2013; accepted 15 Jan 2014; published 7 Feb 2014

39. Z. Shi, W. Liang, J. Luo, S. Huang, B. M. Polishak, X. Li, T. R. Younkin, B. A. Block, and A. K.-Y. Jen, "Tuning the kinetics and energetics of Diels−Alder cycloaddition reactions to improve poling efficiency and thermal stability of high-temperature cross-linked electro-optic polymers," Chem. Mater. **22**(19), 5601–5608 (2010).
40. Y. Enami, C. T. Derose, D. Mathine, C. Loychik, C. Greenlee, R. A. Norwood, T. D. Kim, J. Luo, Y. Tian, A. K.-Y. Jen, and N. Peyghambarian, "Hybrid polymer/sol–gel waveguide modulators with exceptionally large electro–optic coefficients," Nat. Photonics **1**(3), 180–185 (2007).
41. W. S. Zaoui, A. Kunze, W. Vogel, M. Berroth, J. Butschke, F. Letzkus, and J. Burghartz, "Bridging the gap between optical fibers and silicon photonic integrated circuits," Opt. Express **22**(2), 1277–1286 (2014).

1. Introduction

Optical frequency combs are key elements for a multitude of applications such as optical metrology [1], arbitrary-waveform generation [2], and terabit/s communications [3]. In many cases, narrow optical linewidth and the ability to freely choose center wavelength and line spacing are essential. Moreover, dense integration of comb sources along with other devices is important to realize miniaturized systems with high degrees of complexity. This applies especially to high-speed data transmission, where line spacings of tens of GHz are needed for spectrally efficient super-channel transmission with terabit/s data rates [4]. A particularly suitable and versatile approach for integrated frequency comb generation is based on periodic modulation of a continuous-wave (cw) laser with electro-optic phase shifters in an appropriate arrangement [5–8]. In such schemes, the optical linewidth is determined by the cw laser, the line spacing can be adjusted via the modulation frequency, and the number of comb lines depends on the modulation depth and the number of cascaded devices [9–11]. In cases where modulation depth is limited, the bandwidth of the comb spectrum can be increased by inserting the phase modulator in an amplifying feedback loop [12–14]. However, this leads to a restriction of the line spacing due to the round-trip time of the loop, where a resonance condition must be fulfilled. Previous demonstrations of modulator-based frequency combs have mainly focused on using conventional lithium niobate devices [6, 9, 11, 15] along with discrete fiber-optic components. Integrated comb sources have been realized on the InP platform by inserting a phase modulator into an amplifying ring resonator [14]. This arrangement enables generation of 6 lines with a spacing of around 10 GHz and a spectral flatness of 5 dB. However, for many applications, it would be highly desirable to realize miniaturized frequency comb sources on the silicon photonic platform, thereby complementing the already rich portfolio of available devices [16]. One of the main obstacles towards silicon-based comb sources is the limitation associated with currently available phase modulators: Fast modulation is possible with depletion-type pn-junction phase shifters, but these devices feature relatively large voltage-length products $U_\pi L$ of typically more than 10 V mm [17–19]. Injection-type phase shifters, on the other hand, have smaller $U_\pi L$, but modulation bandwidths are limited by the carrier lifetime [20].

In this paper we demonstrate the first modulator-based comb source on a silicon-on-insulator (SOI) substrate. We use the concept of silicon-organic hybrid (SOH) integration [21–25] which combines nanophotonic SOI waveguides with organic cladding materials to realize highly efficient broadband phase shifters [26]. The devices exhibit voltage-length products as small as $U_\pi L$ = 2 V mm at DC. Using a dual-drive Mach-Zehnder modulator (MZM), we demonstrate generation of a flat-top frequency comb comprising 7 lines with a spacing of 40 GHz and a spectral flatness of 2 dB [27]. We demonstrate the viability of SOH comb sources in a series of data transmission experiments, where we explore different line spacings, symbol rates, pulse shapes, and modulation formats. A total line rate of 1.152 Tbit/s and a net spectral efficiency of 4.9 bit/s/Hz are achieved by using a comb with 25 GHz line spacing. In this experiment, 9 carriers are modulated with Nyquist pulses at a symbol rate of 18 GBd using 16-state quadrature amplitude modulation (16QAM) and quadrature phase shift keying (QPSK). In a similar experiment, we reduce the complexity by using QPSK on 7 channels only, thereby enabling transmission over a distance of up to 300 km. For a comb with 40 GHz line spacing and conventional non-return-to-zero (NRZ) QPSK signals, we use a symbol rate of 28 GBd on 9 channels to transmit an aggregate line rate of 1.008 Tbit/s over up to 300 km.

2. SOH modulators for frequency comb generation

The SOH phase shifter [26, 28] consists of an optical slot waveguide [29] electrically connected to copper slotlines through 60 nm thick doped silicon strips. A schematic cross section and simulated mode profile of the optical slot waveguide are depicted in Fig. 1(a). The modulation voltage applied to the electrodes drops across the narrow slot, resulting in a high electric field that strongly overlaps with the optical mode. This leads to highly efficient electro-optic interaction and hence to a low voltage-length product $U_{\pi}L$. The silicon waveguides are fabricated on a SOI wafer with a 2 µm thick buried oxide and a 220 nm thick device layer using 193 nm deep-UV lithography. After processing, the SOI waveguides are covered with the electro-optic chromophore DLD164 [30], which entirely fills the slot. The electro-optic cladding is applied by spin coating and poled at elevated temperatures with a DC voltage applied across the slotline electrodes. More details about the phase shifter can be found in [28]. Our comb generators consist of two phase shifters in a Mach-Zehnder interferometer. These phase shifters are either driven independently in a dual-drive configuration, or in push-pull mode using a single drive signal that induces opposite phase shifts in the two arms. We investigate two MZM types: A 2 mm long dual-drive modulator, and a 1 mm long single-drive device.

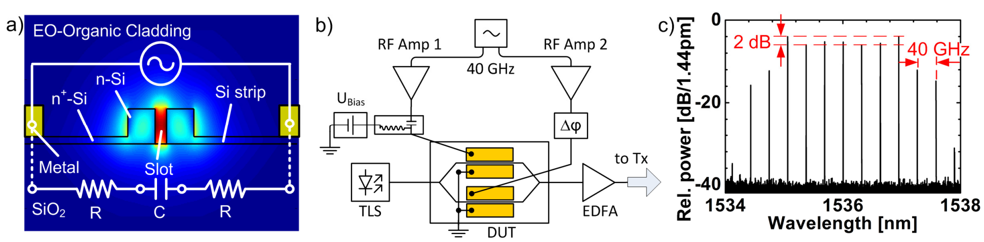

Fig. 1. Dual-drive frequency comb generator and spectrum. (a) Schematic cross-section and simulated optical mode of a silicon-organic hybrid (SOH) phase modulator. The two rails of a silicon slot waveguide are electrically connected to metal electrodes by 60 nm high n-doped silicon strips. The waveguide is covered by an electro-optic cladding material (DLD164), which entirely fills the slot. (b) Integrated dual-drive frequency comb generator: A tunable laser source (TLS) is coupled to a dual-drive SOH Mach-Zehnder modulator (MZM) via grating couplers. The arms are driven by two sinusoidal 40 GHz signals. Flat combs are obtained by carefully adjusting the signal powers and phases along with the bias voltage U_{Bias}. Fiber-chip coupling losses are compensated by an erbium-doped fiber amplifier (EDFA). (c) Flat-top spectrum obtained for electrical drive powers of 28 dBm and 23 dBm measured at the output of the amplifiers, showing 7 lines within 2 dB flatness. The lines are spaced by 40 GHz.

The experimental setup with a dual-drive MZM is shown in Fig. 1(b). A tunable laser source (TLS) is coupled to the chip via grating couplers [31], and the electrodes for the sinusoidal drive signals are contacted with RF probes. The generated frequency comb has a flexible line spacing determined by the modulation frequency. Using sinusoidal drive signals with carefully adjusted amplitude and phase [5], a spectrally flat frequency comb can be generated. The voltage-length product of each phase modulator was measured at DC to be $U_{\pi}L = 2$ V mm. This allows an efficient generation of higher-order optical sidebands with electrical drive powers of approximately 28 dBm and 23 dBm in the respective arms. The resulting optical spectrum is shown in Fig. 1(c). We achieve a spectral flatness of 7 lines within 2 dB. The line spacing amounts to 40 GHz. By comparing the measured optical spectrum to simulations, we estimate the peak-to-peak modulation depth in the two MZM arms to be 3.6π and 2.7π, respectively. The phase difference of about π matches nicely to theoretical predictions for an optimally flat comb [5].

Spectrally flat frequency combs are advantageous for WDM transmission, since low-power lines are avoided and all WDM channels have the same signal quality. However, the use of a single-drive MZM simplifies the experimental setup considerably, because only one electrical amplifier is needed. A single-drive device is demonstrated using the setup depicted in Fig. 2(a). For the push-pull device, the voltage-length product of each individual phase modulator amounts to $U_{\pi}L = 2$ V mm. Figure 2(b) shows the comb spectrum generated by an electrical drive signal with a frequency of 25 GHz and a power of 23 dBm measured at the output of the amplifier. The spectrum has 7 lines within a power range of 10 dB. Figure 2(c) shows the optical spectrum generated with a 40 GHz drive signal. Here, a slightly higher amplifier output power of 29 dBm is used to overcome the frequency-dependent increase of electrode losses and to enable larger optical bandwidth. We obtain a comb featuring 7 lines with a flatness of 7 dB. In contrast to the dual-drive comb generator, the spectral flatness cannot be optimized by adjusting the drive parameters, and an external optical filter is required to obtain flat-top comb spectra, see Section 3.2. As the dual-drive MZM chip broke during preliminary data transmission experiments, we continued the experiments with single-drive devices.

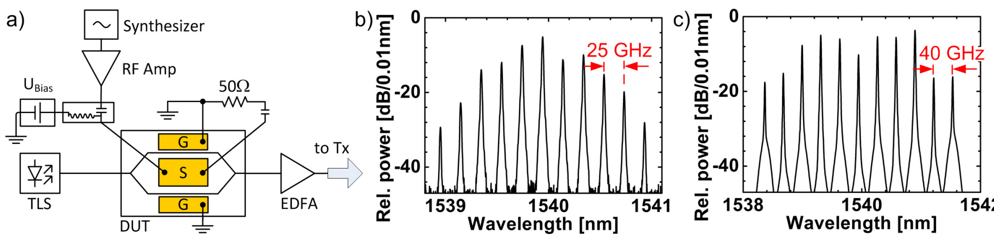

Fig. 2. Single-drive frequency comb generator and spectra. (a) Schematic of the single-drive push-pull frequency comb generator: A tunable laser source (TLS) is coupled to the SOH MZM via grating couplers. The device is driven by sinusoidal signals of different frequencies, thereby defining the line spacing of the generated comb. The operation point can be chosen with the bias voltage U_{Bias}. The electrodes are terminated with 50 Ω. Fiber-chip coupling losses are compensated by an erbium-doped fiber amplifier (EDFA). (b) Resulting optical spectrum using an electrical drive signal of 25 GHz and a RF power of 23 dBm, yielding 7 lines with a spectral flatness of 10 dB. (c) Resulting optical spectrum using an electrical drive signal of 40 GHz and a RF power of 29 dBm, yielding 7 lines with a spectral flatness of 7 dB.

All generated combs feature excellent wavelength stability of ± 2.5 pm and linewidths in the order of 100 kHz, solely governed by the cw laser. The line spacing is determined to an accuracy of better than 10^{-9} by the synthesizer that is used to drive the modulators. The stability of the power per line is mainly given by the ability to maintain constant driving conditions. Since the modulators were operated without thermal stabilization at relatively high optical and electrical power levels, it was necessary to manually adjust the bias voltage in intervals of several minutes to compensate thermal drift and to preserve the spectral envelope of the comb. Bias point drift can be overcome by temperature stabilization of the device or by electronic feedback control.

3. Terabit/s data transmission using SOH frequency comb sources

To demonstrate the viability and the flexibility of SOH frequency comb sources, we perform a series of data transmission experiments using different symbol rates, pulse shapes, and modulation formats. For maximum spectral efficiency, dense line spacing of 25 GHz is used in combination with Nyquist pulse shaping. This allows generation of a data stream with an aggregate line rate of 1.152 Tbit/s and a spectral efficiency of 4.9 bit/s/Hz. The experiment was performed with a single-drive push-pull device, resulting in comb lines with noticeable

#200735 - $15.00 USD Received 7 Nov 2013; accepted 15 Jan 2014; published 7 Feb 2014

power differences. A homogeneous power distribution among the optical channels can be achieved by using a programmable optical filter for spectral flattening. In combination with more robust QPSK modulation, this enables transmission of a 504 Gbit/s data stream over a distance of up to 300 km. In simpler transmission schemes where spectral efficiency is not of prime importance, conventional NRZ pulses may be used in combination with larger channel spacing. We generate a line spacing of 40 GHz by simply increasing the modulation frequency of our comb source, allowing transmission of 28 GBd NRZ-QPSK signals without undue cross talk between neighboring channels. Using this scheme, we demonstrate transmission with an aggregate line rate of 1.008 Tbit/s over up to 300 km.

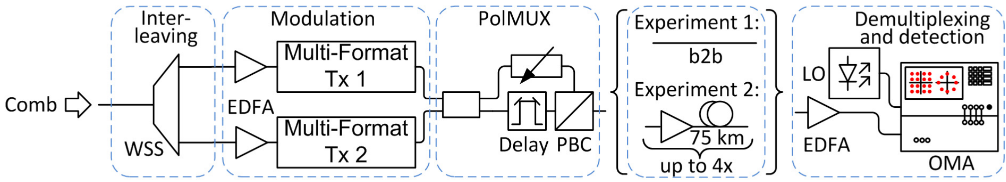

Fig. 3. Data transmission setup. A wavelength-selective switch (WSS) splits the comb into even and odd carriers which are modulated independently in a multi-format transmitter. The two sets of channels are recombined, and polarization multiplexing (PolMUX) is emulated by creating time-shifted copies of the data stream and merging them on orthogonal polarizations. Experiment 1: In a first experiment, the data is fed directly into the receiver (back-to-back, b2b). Experiment 2: Up to 4 spans of 75 km SMF are used for transmission over up to 300 km. At the receiver, the signal is amplified and the channels are demultiplexed and detected by an optical modulation analyzer (OMA). A free-running external cavity laser acts as a local oscillator (LO) for coherent reception.

3.1 Generation of Terabit/s data streams using dense combs and Nyquist pulse shaping

To generate a data stream with high spectral efficiency, we use the experimental setup shown in Fig. 3. The frequency comb is obtained from a single-drive push-pull MZM driven by a 25 GHz sinusoidal signal, see Fig. 2(b) for the raw comb spectrum prior to data modulation. A programmable optical filter (Finisar WaveShaper, wavelength selective switch, WSS) is then used to separate even and odd carriers, which are modulated with independent pseudo-random bit sequences (PRBS) of length $2^9 - 1$. Modulation is done by multi-format transmitters, generating Nyquist pulses [32] at a symbol rate of 18 GBd and enabling a wide variety of different modulation formats [33]. Polarization-division multiplexing (PDM) is emulated by splitting the data stream, delaying one part with respect to the other, and merging them in a polarization beam combiner on orthogonal polarization states. The signal is received and characterized by an optical modulation analyzer (OMA, Agilent N4391A) with a free-running external cavity laser as local oscillator (LO). Digital signal processing is performed for polarization demultiplexing and equalization. We record the constellation diagrams and extract the error vector magnitude (EVM) as a measure for signal quality for each channel and each polarization.

The results are depicted in Fig. 4. The strongest carriers 2 … 8 were suitable for PDM-16QAM modulation, whereas the two weakest carriers 1 and 9 supported PDM-QPSK signals only. All channels show measured bit error ratios (BER) better than 4.3×10^{-3}, which is below the hard-decision forward-error correction (FEC) threshold of 4.5×10^{-3} [34]. The aggregate line rate is 1.152 Tbit/s. Taking into account a 6.7% overhead for the hard-decision FEC, we obtain a net spectral efficiency of 4.9 bit/s/Hz. In the current experiment, we chose a line spacing of 25 GHz, which is in accordance with standards recommended by the International Telecommunication Union [35]. In principle, this would enable a symbol rate of 25 GBd per channel, since no spectral guard band is needed for Nyquist-WDM [36]. However, the actual symbol rate was limited to 18 GBd by our current transmitter hardware. As a consequence, parts of the spectrum had to remain unused, thus offering potential for further increasing spectral efficiency in future experiments. Transmission of the signal over large distances was not possible due to insufficient BER margin, which was mainly caused by

#200735 - $15.00 USD Received 7 Nov 2013; accepted 15 Jan 2014; published 7 Feb 2014

the rather high on-chip insertion loss of the modulator amounting to approximately 21 dB. We attribute this loss to an imperfect fabrication of the multi-mode interference couplers used in the MZM. With improved fabrication steps we would expect an on-chip loss of around 6 dB.

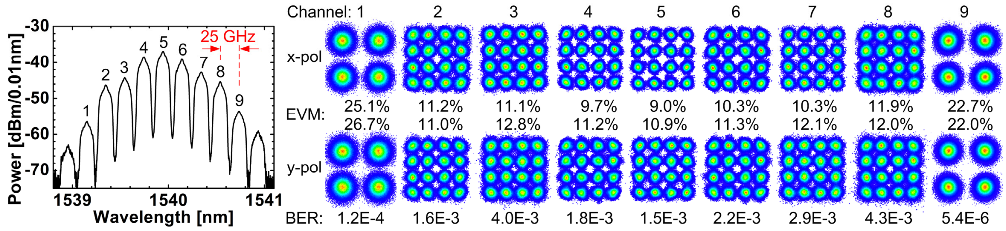

Fig. 4. Results of back-to-back data transmission. A total of 9 carriers spaced by 25 GHz were generated by an integrated SOH comb source. Optical spectrum of the modulated carriers (left) and constellation diagrams (right) for all channels and both polarizations are depicted along with measured EVM values. The 7 strongest carriers were modulated with Nyquist pulse-shaped 16QAM signals, whereas QPSK was used for weaker carriers 1 and 9. The symbol rate is 18 GBd. We obtain BER values below the hard-decision threshold for all channels, yielding an aggregate line rate of 1.152 Tbit/s.

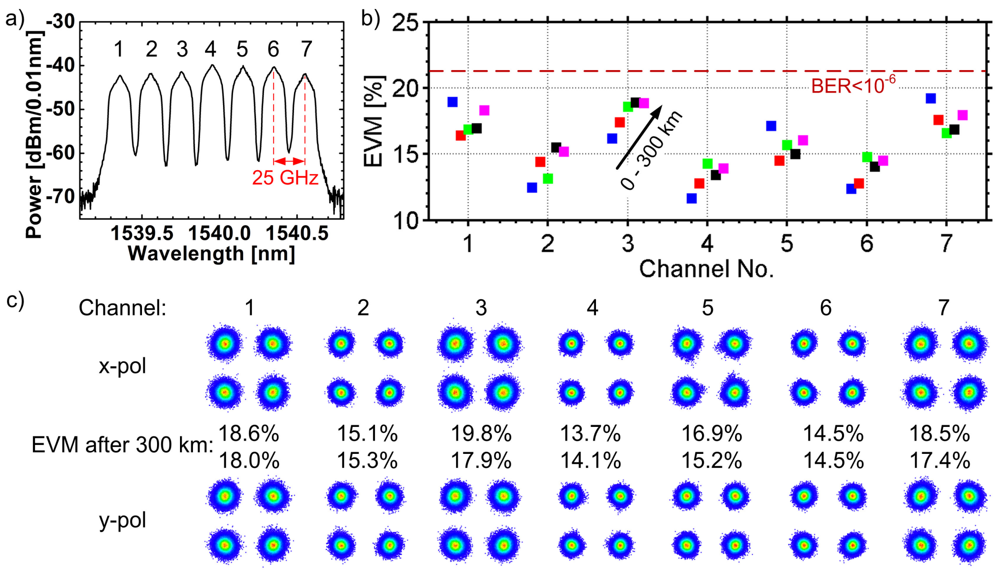

Fig. 5. Results for data transmission of QPSK signals: (a) Optical spectrum of the modulated carriers. The 7 strongest carriers are spectrally flattened by the WSS. (b) The average EVM of both polarizations over channel number are shown color-coded (and slightly offset for clarity of presentation) for each length of fiber span (0 km, 75 km, 150 km, 225 km, 300 km). Drift of the operation point of the integrated comb source leads to some deviations from equal optical power for each channel, but BER below 10^{-6} are achieved for all channels nonetheless. (c) Constellation diagrams of all 7 channels and both polarizations after 300 km transmission.

3.2 Transmission of a Nyquist-WDM signal with spectrally flattened comb

To improve the signal quality of the data transmission, the experiment was repeated using QPSK and the 7 strongest lines, which were in addition spectrally flattened with the WSS for a more homogeneous channel performance. For this experiment, we use a different comb generator with a voltage-length product of $U_\pi L$ = 3.2 V mm at DC, which is slightly larger than the value for the devices used in the previous section. All carriers were modulated with sinc-shaped Nyquist pulses at a symbol rate of 18 GBd using PDM-QPSK signals. The

#200735 - $15.00 USD Received 7 Nov 2013; accepted 15 Jan 2014; published 7 Feb 2014

resulting spectrum consists of 7 channels with similar optical power, Fig. 5(a). In Fig. 5(b), the average error vector magnitudes (EVM) of both polarizations are shown for all channels and all transmission distances (0 km, 75 km, 150 km, 225 km, 300 km). The EVM of all channels are smaller than 21.2%, which corresponds to a BER of 10^{-6} and is indicated by a dashed red line in Fig. 5(b) [37]. Figure 5(c) shows the constellation diagrams of all channels and both polarizations after transmission over 300 km. The demonstrated line rate amounts to 504 Gbit/s. The operation point of the comb generator was not stabilized, leading to some residual drift. This drift caused variations in channel performance during the measurements. A bias stabilization scheme could avoid this impairment in future experiments.

3.3. Terabit/s WDM transmission using NRZ-QPSK

To demonstrate data transmission with conventional NRZ pulses and symbol rates of 28 GBd, we increase the line spacing of our comb to 40 GHz. The comb spectrum comprises 9 lines that are usable for data transmission, see Fig. 2(c). The optical spectrum of the modulated carriers can be seen in Fig. 6(a). Figure 6(b) depicts the average EVM of both polarizations for all channels and various transmission distances (0 km, 75 km, 150 km, 225 km, 300 km). The EVM of all channels is below the threshold for hard-decision FEC, which corresponds to a BER of 4.5×10^{-3} and is represented by the red dashed line in Fig. 6(b) [37]. The total line rate amounts to 1.008 Tbit/s. As before, slight variations in channel performance during the measurements are caused by drift of the operating point and can be mitigated by using electronic bias point stabilization in future experiments.

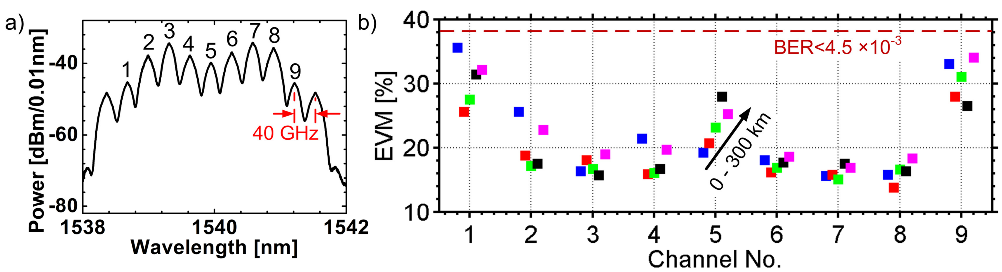

Fig. 6. Results for data transmission of NRZ QPSK signals: (a) Optical spectrum of the modulated carriers for 40 GHz spacing and 29 dBm of RF power measured at the output of the drive amplifier. (b) Average EVM of both polarizations over channel number. The results obtained for different fiber spans (0 km, 75 km, 150 km, 225 km, 300 km) are color-coded and slightly offset for clarity of presentation. Drift of the operating point of the comb source leads to variations of the BER obtained for different transmission distances. Nonetheless, BER values below the hard-decision threshold of 4.5×10^{-3} are achieved for all channels, yielding a gross line rate of 1.008 Tbit/s.

4. Future research directions

A key aspect of SOH devices is the long-term stability of the poling-induced molecular order. The material used for the current experiments consists of a rather loose arrangement of DLD164 electro-optic chromophores and hence has a relatively low glass transition temperature of only 66°C. This limits the on-chip power dissipation. In our experiments, the devices were operated at lasers powers of up 18 dBm, measured in the input fiber, which corresponds to 12 dBm of on-chip laser power, taking into account typical fiber-chip coupling losses of 6 dB. At the same time, up to 28 dBm of RF power was continuously coupled to the chip. Still, even at these power levels, the material was stable enough to enable the presented experiments under ambient atmosphere in a normal lab environment.

We expect that stability of the electro-optic material can be significantly improved by synthetically modified DLD164 chromophores that bear specific crosslinking agents for post-poling lattice hardening. The viability of this approach has already been demonstrated for similar classes of electro-optic compounds, yielding materials being stable for temperatures of

#200735 - $15.00 USD Received 7 Nov 2013; accepted 15 Jan 2014; published 7 Feb 2014

up to 250 °C [38,39]. It has also been demonstrated experimentally that these techniques can be applied to realize temperature-stable all-polymeric MZM [40]. For DLD164, the addition of crosslinking agents to the side groups can be realized without affecting the electro-optic activity of the chromophore or the interaction of the side chains. This is subject to ongoing research.

Moreover, the insertion loss of the device is currently limiting its practical applicability. In addition to approximately 6 dB of fiber-chip coupling loss per interface, the device features an on-chip loss of approximately 21 dB. Moreover, modulation distributes the incoming power over many spectral lines, resulting in typical output powers between −27 dBm and −17 dBm per comb line, measured in the fiber immediately after the modulator. We expect that the overall insertion losses can be reduced dramatically by systematic optimization of fiber-chip coupling [41], and by improving device design and fabrication.

5. Summary and conclusion

We demonstrate modulator-based frequency comb generators fabricated on the silicon-organic hybrid (SOH) platform. Using a dual-drive MZM, we generate flat-top frequency combs featuring 7 lines with a spacing of 40 GHz and a spectral flatness of 2 dB. This performance can well compete with integrated InP-based comb generators, where a phase modulator inside an amplifying ring was used to demonstrate 6 lines with a spacing of around 10 GHz and a spectral flatness of 5 dB. The viability of the SOH comb generators is confirmed in a series of data transmission experiments, where we demonstrate line rates of more than 1 Tbit/s and transmission distances of up to 300 km. Spectral efficiencies of up to 4.9 bit/s/Hz are achieved by using 16QAM signals along with a line spacing of 25 GHz and Nyquist pulse shaping at a symbol rate of 18 GBd. We believe that SOH comb sources can become essential elements within the already rich silicon photonic device portfolio.

Acknowledgments

This work was supported by the European Research Council (ERC Starting Grant ‘EnTeraPIC’, number 280145), by the Alfried Krupp von Bohlen und Halbach Foundation, by the Karlsruhe School of Optics & Photonics (KSOP), by the Center for Functional Nanostructures (CFN), by the Helmholtz International Research School for Teratronics (HIRST), by the Initiative and Networking Fund of the Helmholtz Association, by the Karlsruhe Nano-Micro Facility (KNMF), and by the EU-FP7 projects SOFI, OTONES, and PHOXTROT. We further acknowledge support by the Open Access Publishing Fund of Karlsruhe Institute of Technology (KIT).